Supplementary Information for

Modulating the contact properties of XY_2/Sc_2CCl_2 (X = Nb, Ni, Ti, V, Mn, Ta; Y = S, Se) heterostructures via layer number, electric field, and vertical strain

You Xie*, Miao Zhang, Zheng-Yong Chen, Chen Du, Jia-Qi Li, Yan Chen, Li-Mei Hao, Tao Zhang

College of Sciences, Xi'an University of Science and Technology, Xi'an 710054, China

* Corresponding author.

E-mail address: xieyou@hotmail.com (Y. Xie).

Outline

S1. Electron localization function of monolayer Sc_2CCl_2

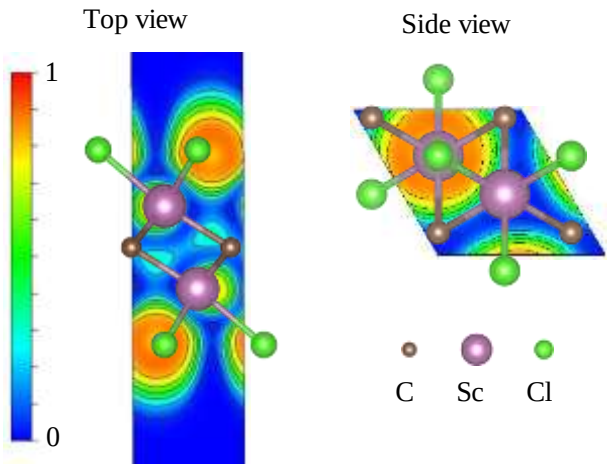

Fig. S1. Electron localization function of monolayer Sc_2CCl_2.

S2. AIMD simulation results for the XY_2/Sc_2CCl_2 (X = Nb, Ni, Ti, V, Mn, Ta; Y = S, Se) vdWHs

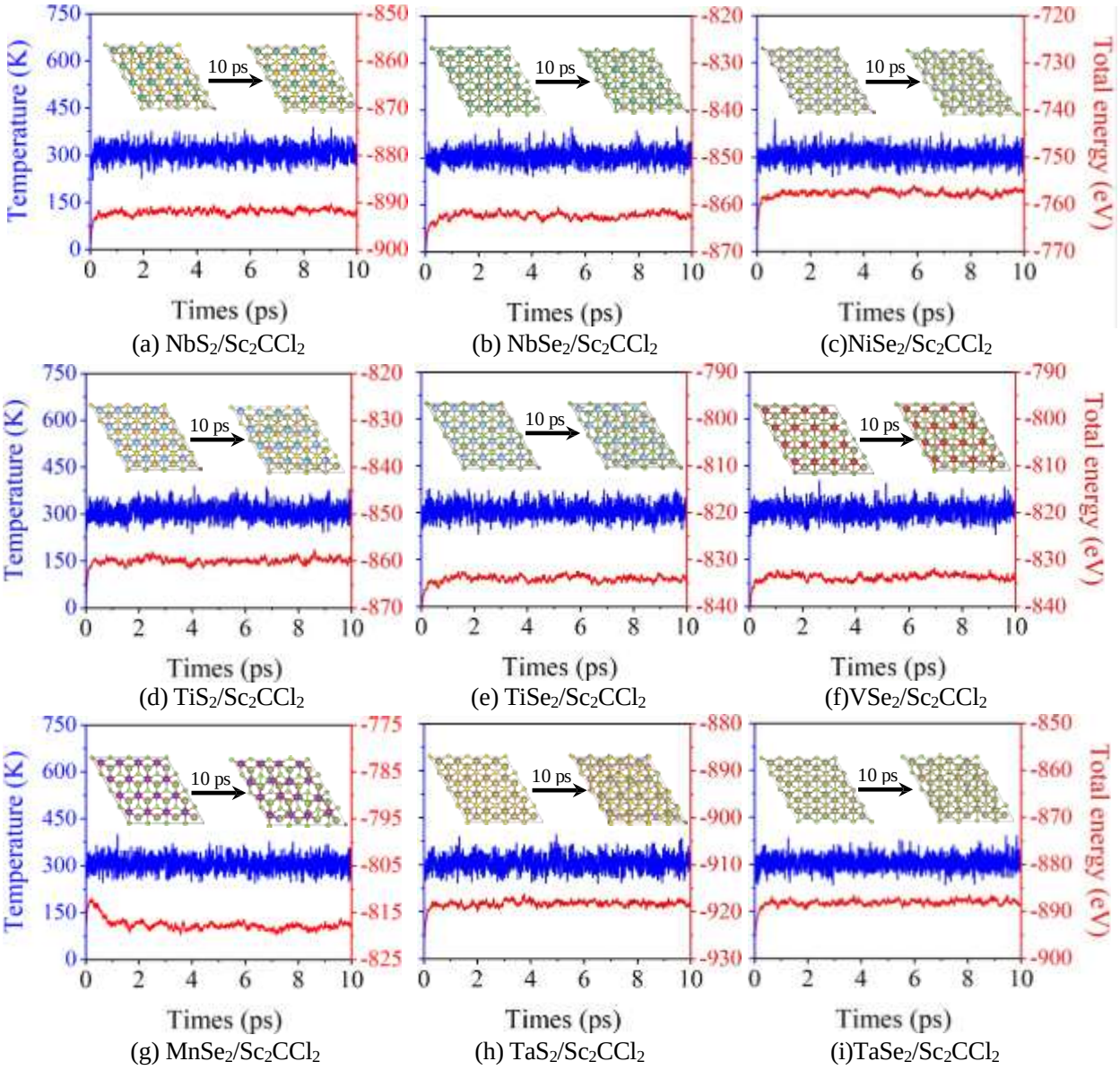

Fig. S2. Ab initio molecular dynamics (AIMD) simulation results for the XY_2/Sc_2CCl_2 (X = Nb, Ni, Ti, V, Mn, Ta; Y = S, Se) vdWHs.

S3. Electrostatic potential of the XY_2/Sc_2CCl_2 (X = Nb, Ni, Ti, V, Mn, Ta; Y = S, Se) vdWHs.

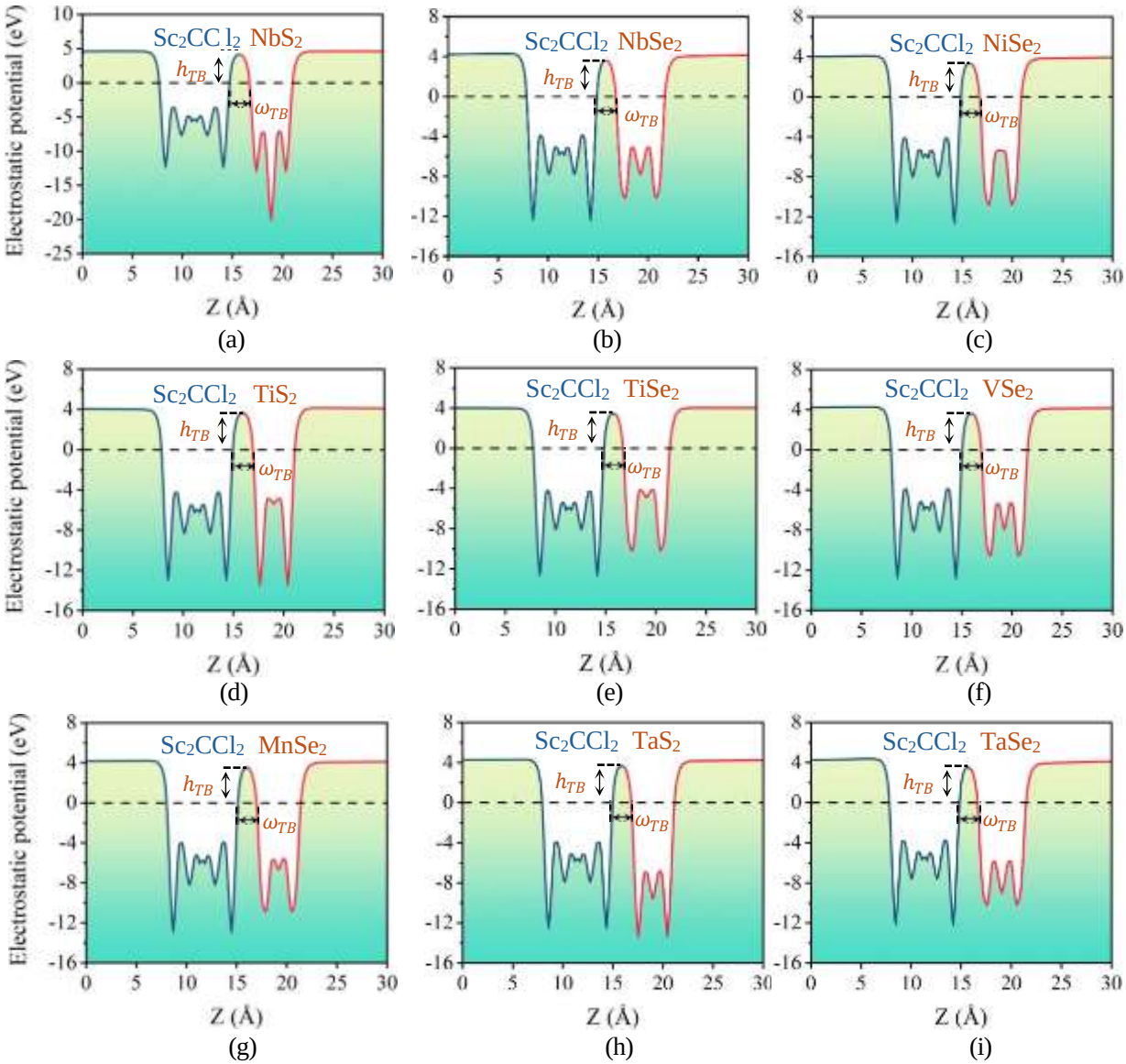

Fig. S3. Electrostatic potential of the XY_2/Sc_2CCl_2 (X = Nb, Ni, Ti, V, Mn, Ta; Y = S, Se) vdWHs.

h_{TB} and ω_{TB} are extracted from the planar-averaged potential profile along Z. h_{TB} is the energy difference between the potential peak and Fermi level; ω_{TB} is the lateral distance over which the potential remains above Fermi level, bounded by the points where it first rises above and finally decays back to Fermi level.

S4. Evolution of the electrostatic potential for XY_2/Sc_2CCl_2 vdWHs under a vertical electric field

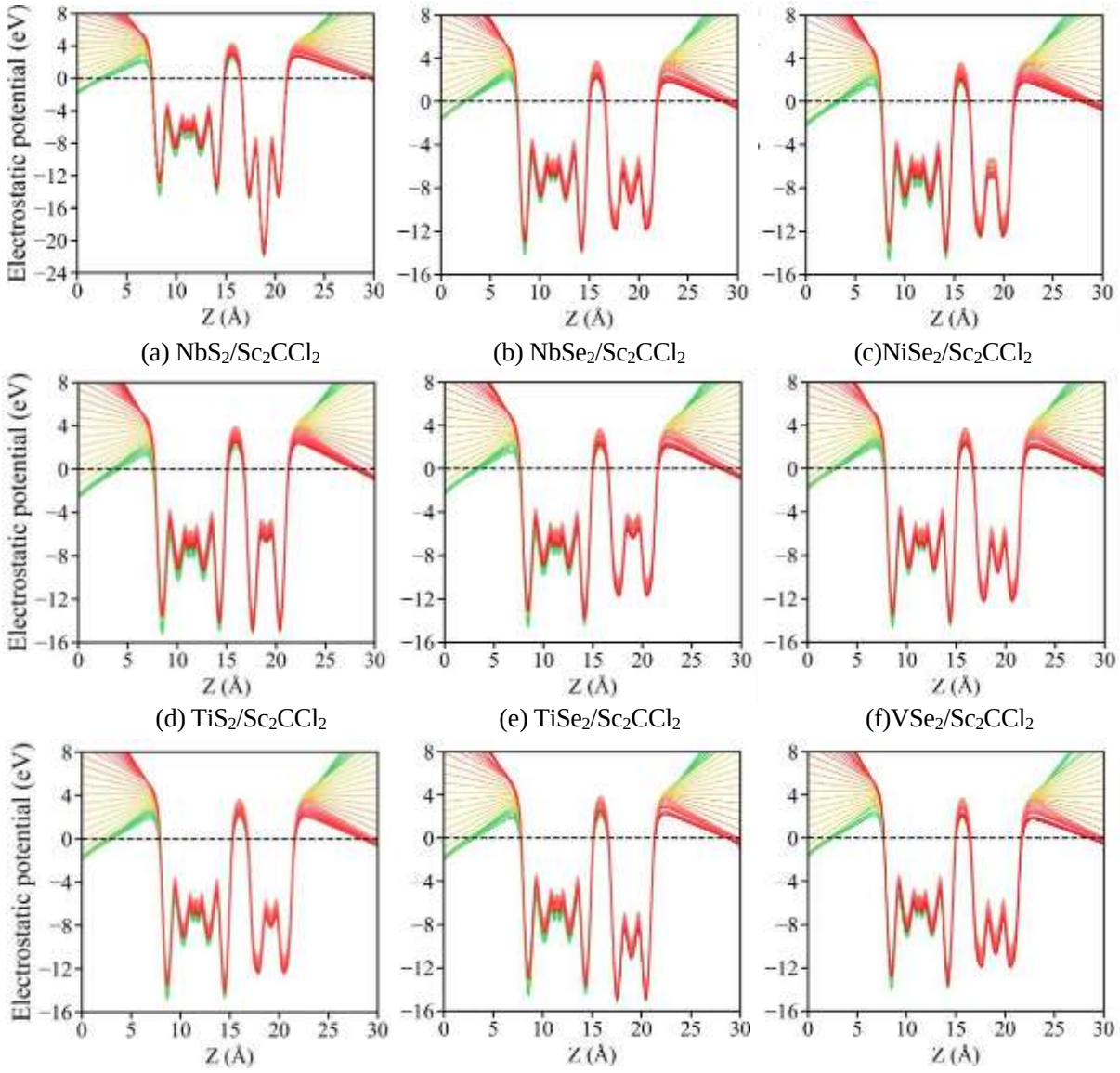

Fig. S4. Evolution of the electrostatic potential for XY_2/Sc_2CCl_2 vdWHs under a vertical electric field.

The essence of electric field modulation lies in altering the interfacial electrostatic potential distribution to modify the band structure. Fig. S4 shows the evolution of the electrostatic potential for different heterostructures under an applied electric field. Under zero field, all systems exhibit typical Schottky barrier characteristics. Under a positive electric field (where the curve color in the electrostatic potential plots changes from red to green, corresponding to the transition from $E > 0$ to $E < 0$), the height of the interfacial potential step increases, which elevates the SBH by shifting the semiconductor's band edges away from Fermi level.

S5. Evolution of MIGS Weight with electric field

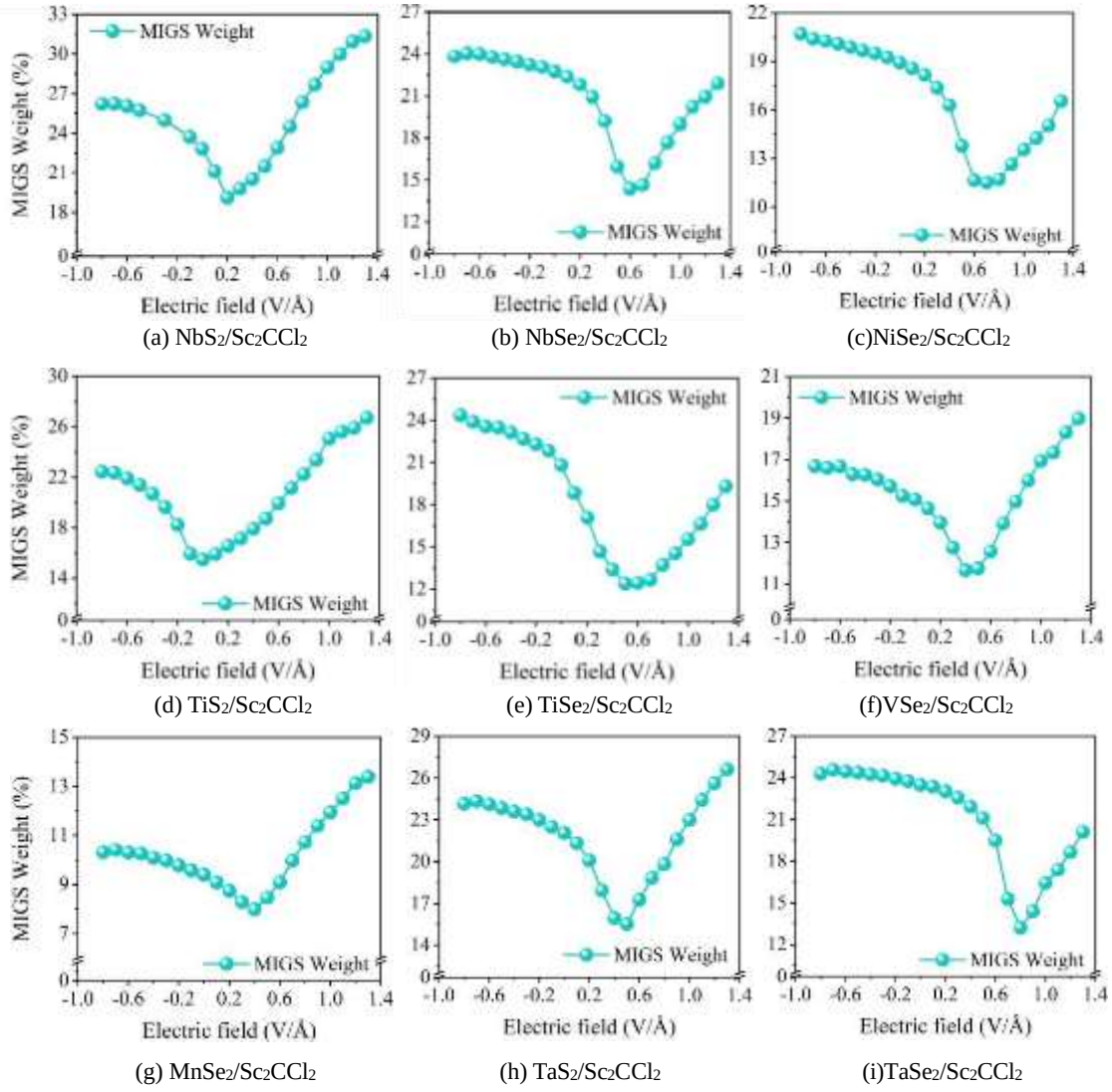

Fig. S5. Variation in MIGS weight with electric field for XY_2/Sc_2CCl_2 heterostructures.

We systematically investigated the behavior of metal-induced gap states for all nine XY_2/Sc_2CCl_2 heterostructures under an applied vertical electric field by calculating the density of states within a specified energy window (corresponding to the band gap region of the intrinsic semiconductor Sc_2CCl_2) near the interface. The results reveal significant and tunable variations in the MIGS proportion. Overall, as the electric field increases from negative to positive values, all systems exhibit a non-monotonic trend where the MIGS proportion first decreases and then increases (see Fig. S5). The physical origin of this universal trend is closely related to the modulation of the intrinsic built-in electric field at the heterostructure interface by the external field. At zero external field, a built-in electric field exists at the interface due to the work function difference between the metal and semiconductor, leading to band bending on the semiconductor side and an intrinsic

distribution of MIGS. When an external field opposite to the built-in field is applied (e.g., a positive field in this study, as the intrinsic field points from the metal to the semiconductor), it counteracts part of the built-in field, reducing the degree of band bending and making the barrier profile on the semiconductor side steeper. This shortens the decay length of the metal electron wavefunctions into the semiconductor gap, thereby decreasing the MIGS density within the gap. When the external field reaches a certain value, it may maximinally flatten the bands near the interface, at which point the MIGS proportion reaches its minimum. Conversely, when an external field aligned with the built-in field is applied, it enhances the total effective field, increases band bending, widens or alters the barrier region, and slows the decay of metal electronic states, leading to a subsequent increase in MIGS density. Therefore, our data and analysis directly confirm that MIGS not only exist but are also key interface states that can be dynamically and continuously tuned by an external electric field. Their initial decrease followed by an increase essentially reflects the counteraction and enhancement of the intrinsic built-in field by the external field, which in turn modulates the degree of band bending and thereby controls MIGS—a primary physical origin of Fermi-level pinning.

S6. Evolution of the electrostatic potential for XY_2/Sc_2CCl_2 vdWHs under vertical strain.

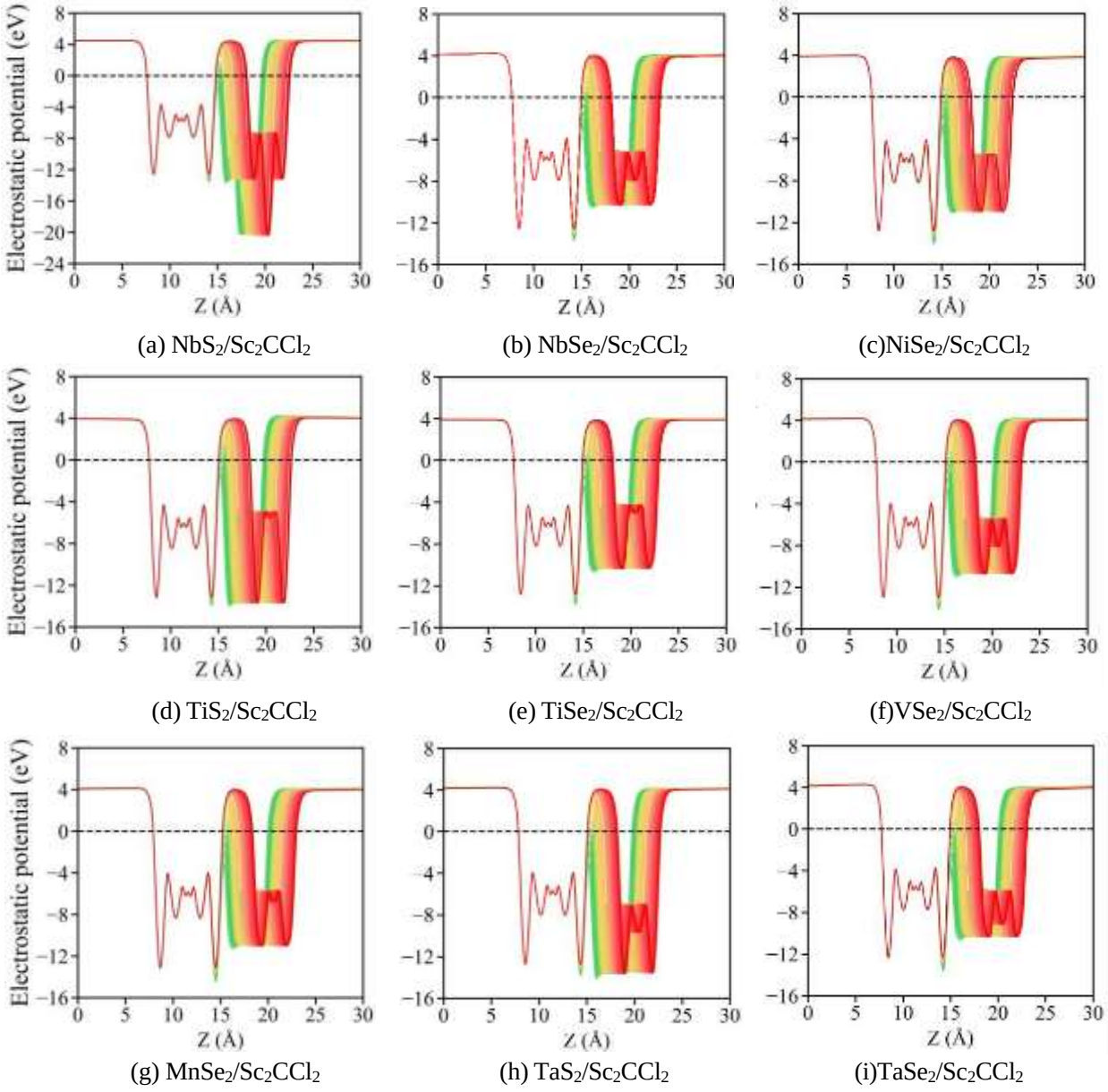

(a) NbS_2/Sc_2CCl_2 (b) $NbSe_2/Sc_2CCl_2$ (c)$NiSe_2/Sc_2CCl_2$

(d) TiS_2/Sc_2CCl_2 (e) $TiSe_2/Sc_2CCl_2$ (f)VSe_2/Sc_2CCl_2

(g) $MnSe_2/Sc_2CCl_2$ (h) TaS_2/Sc_2CCl_2 (i)$TaSe_2/Sc_2CCl_2$

Fig. S6. Evolution of the electrostatic potential for XY_2/Sc_2CCl_2 vdWHs under vertical strain.

To gain a deeper, microscopic understanding of the modulation mechanism of vertical strain on the interfacial electronic structure, we systematically plotted the electrostatic potential distribution curves for all vdWHs at different D values, as shown in Fig. S6. The evolution of the electrostatic potential in the direction perpendicular to the interface intuitively reveals the formation and variation of built-in electric field, which is key to analyzing the origin and evolution of the Schottky barrier. Under zero vertical strain, all vdWHs exhibit typical Schottky barrier characteristics. With the application of vertical strain, the electrostatic potential distribution at the interface shifts

systematically. Under compressive strain (where the curve color in the electrostatic potential plots changes from red to green, corresponding to the transition from tensile ($\Delta D > 0$) to compressive ($\Delta D < 0$) strain), the electronic interaction between the XY_2 and Sc_2CCl_2 layers is significantly enhanced, triggering more intense interfacial charge rearrangement and a larger interface dipole moment. The resulting potential difference increases markedly, and the effective Schottky barrier is significantly lowered, causing a sharp rise in the TP. Conversely, when tensile strain is applied, the interlayer coupling is weakened. The electrostatic potential curves indicate that the strength of the interface dipole consequently diminishes, increasing the effective width of the tunneling barrier. This becomes the dominant factor leading to the significant decrease in the TP under tensile strain.

S7. Evolution of MIGS Weight under vertical strain

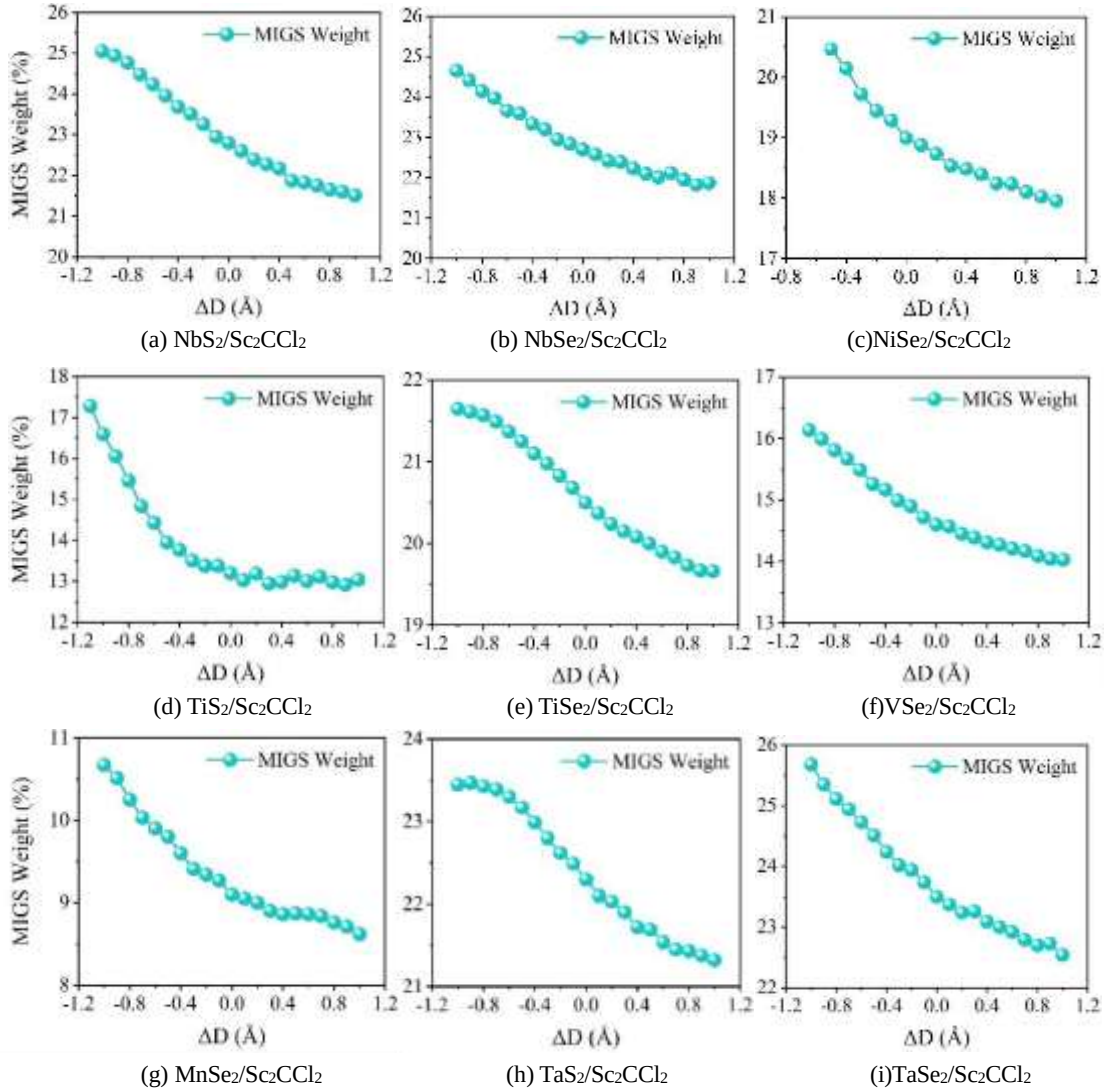

(a) NbS_2/Sc_2CCl_2 (b) $NbSe_2/Sc_2CCl_2$ (c)$NiSe_2/Sc_2CCl_2$

(d) TiS_2/Sc_2CCl_2 (e) $TiSe_2/Sc_2CCl_2$ (f)VSe_2/Sc_2CCl_2

(g) $MnSe_2/Sc_2CCl_2$ (h) TaS_2/Sc_2CCl_2 (i)$TaSe_2/Sc_2CCl_2$

Fig. S7. Variation in MIGS weight with interlayer spacing change (ΔD) for XY_2/Sc_2CCl_2 heterostructures.

We further examined the modulation of interfacial MIGS by vertical strain. The data shows a clear trend: the MIGS proportion generally decreases as the interlayer distance increases (see Fig. S7). The physical origin of this systematic trend lies in the fact that vertical strain directly modulates the strength of interlayer coupling. The nature of MIGS is the exponential decay and extension of metal electron wavefunctions into the semiconductor band gap. Their spatial distribution and density are strongly dependent on the wavefunction overlap at the metal-semiconductor interface. Under compressive strain, the reduced interlayer distance significantly increases the spatial overlap between the atomic orbitals of the metal and semiconductor. This enhances the interfacial wavefunction coupling, making it easier for electron states near the metal Fermi level to 'penetrate' into the semiconductor gap region. This results in a relatively longer decay

length for MIGS or an increased integrated density of states within the given energy window, manifesting as a higher MIGS proportion. Under tensile strain, the increased interlayer distance weakens interlayer electronic coupling. The decay of metal wavefunctions into the semiconductor side accelerates, reducing the tail state density formed within the semiconductor gap, which consequently leads to a decrease in the MIGS proportion.